

Measurement of Blade Deflection of an Unmanned Intermeshing Rotor Helicopter

Andreas E. Voigt

Research scientist

DLR

Braunschweig, Germany

Johann C. Dauer

Research scientist

DLR

Braunschweig, Germany

Florian Knaak

Graduate student

DLR

Braunschweig, Germany

ABSTRACT

The dynamic behavior of intermeshing rotor blades is complex and subjected to rotor-rotor-interactions like oblique blade-vortex and blade-wake interactions. To gain a better understanding of these effects a blade deflection measurement method is proposed in this paper. The method is based on a single camera per rotor blade depicting the rotor blade from a position fixed to the rotor head. Due to the mounting position of the camera close to the rotational plane the method is called In-Plane Blade Deflection Measurement (IBDM). The basic principles, data processing and measurement accuracy are presented in the paper. The major advantages of the proposed method are the applicability to both, flight and wind tunnel trials, as well as the usability for multi-rotor configurations having a significant rotor overlap. Furthermore comparisons to other blade deflection measurement methods are presented. Finally, experimental data of a flight test of an unmanned intermeshing helicopter is presented.

NOTATION

A	Rotor area, $A=\pi R^2$, m^2
c	Profile chord length, m
C_T	Thrust coefficient, $C_T = P/(\rho_\infty A(\Omega R)^2)$
N_B	Number of blades
P	Power, W
R	Rotor radius, m
V_∞	Freestream velocity, m/s
α	Angle of attack of the rotor, rad
Θ_L	Lateral pitch angle, $degrees$
Θ_S	Longitudinal pitch angle, $degrees$
Θ_0	Collective pitch angle, $degrees$
μ	Advance ratio, $\mu=V_\infty \cos\alpha/(\Omega R)$
μ_z	Axial advance ratio, $\mu_z = \mu \tan\alpha$
ρ_∞	Density of air, kg/m^3
σ	Rotor solidity, $\sigma = N_B c / (\pi R)$
Ω	Rotor rotation frequency, rad/s

INTRODUCTION

Detailed knowledge of the blade deflections is crucial when it comes to validation of high fidelity rotor codes or to determine rotor and rotor blade design characteristics. This kind of data is rare for conventional rotor configurations [1] [2] [3] [4]. For non-

conventional rotor configurations such data is even rarer and only wind tunnel measurements of a coaxial rotor configuration are published in [5]. These non-conventional rotor configurations like coaxial or intermeshing rotors exhibit an inherent rotor-rotor-interaction as well as oblique blade-vortex interactions. These dynamic effects lead to more complex and dynamic air loads compared to conventional configurations and could significantly influence the blade deflection. To assess such effects and obtain a deeper understanding of the dynamic behavior a blade deflection measurement method for intermeshing rotor configurations is presented in this paper.

Most of the previously proposed measurement methods to determine rotor blade deflections are not usable for rotor configurations with more than one rotor that have a significant rotor-to-rotor overlap. Those methods often use ground-based cameras and therefore suffer from blind spots due to rotor overlap or caused by the fuselage. Additionally, these optical methods are rarely employed in flight test due to the general set-up of the cameras. In-flight measurements often use highly instrumented rotor blades, specifically designed for such tests. However, if serially produced rotor blades are used such methods are not usable.

Therefore, a new and simple measurement method was developed to assess the rotor blade deflections for wind tunnel and free flight applications independent of the rotor configuration. Another requirement is the measurement of the blade deflection at any rotor azimuth and optionally the usage of serially produced blades instead of specifically instrumented and built rotor blades.

The proposed method uses a mono camera mounted in the rotor disc plane depicting the rotor blade while spinning with it. The rotor blade is equipped with several marker pairs at defined radial positions to calculate blade flap, lead-lag and torsional motion from the images taken. This set-up is used for each blade of an instrumented rotor head.

The remainder of the paper is structured as follows: first, an overview of blade deflection measurement methods is provided. Then, the basic principles of the proposed method are introduced. Next, application of the In-Plane Blade Deflection Measurement (IBDM) method to an unmanned intermeshing helicopter is presented and the calibration process is described. In the following chapter, a comparison to other blade deflection measurement methods is given including an accuracy and error calculation based on real flight test data. Finally, flight test results are discussed and the results summarized.

RELATED WORK: BLADE DEFLECTION MEASUREMENT METHODS

For isolated rotors, propellers and rotors without overlap a variety of methods have been developed to measure the blade deflection of the rotating blades. These measurements have been used in wind tunnel and flight experiments. In the following section an overview of these methods is provided.

Stereo Pattern Recognition (SPR) Methods

The SPR methods use at least two cameras located out of the plane of rotation. The cameras are in a fixed position and need an overlapping field of view [1]. The SPR uses an array of optical markers on the rotor blades to determine the blade deflection. This method is widely used in wind tunnel applications and also known as Blade Deflection (BD) measurement [6] [2] or three-dimensional point tracking (3DPT) [4]. For in-flight measurements of rotor blade deflections this approach is not well suited due to the distance needed between the rotor and the camera to depict a significant part of the rotor disk. It can be used to assess the blade deflection, in principle. However, it is limited to hover in ground effect as demonstrated with a Robinson R44 helicopter [4]. For rotors with overlap this method could be adapted to use rotor-specific markers. But with this modification a 360° azimuth coverage is not possible due to the overlapping of the rotors themselves or with the helicopter fuselage.

If there is just one rotor and sufficient space along the rotational axis, a very similar approach can be used to measure the blade deflection referred to as Image Pattern Recognition Technique (IPCT) [7]. This method uses at least two cameras moving with the rotor blade. The cameras are mounted in the rotational axis of the

rotor and with an optical inclination angle of up to 75° to the normal vector of the blade surface at the blade tip. However, this method is not usable for rotors with significant overlap like the intermeshing rotor due to the very limited space along the rotational axis of the rotor. Another method suitable for coaxial rotors is known as Blade Deformation Measuring System (BDMS). It uses one or two cameras mounted elevated and rotating with the rotor very similar to the IPCT approach [5]. It also uses blade markers mounted on the rotor blade. However, this system is not usable for an intermeshing rotor due to its elevation over the rotor disk and the subsequent aerodynamic influence on the flight behavior during in-flight measurements. The BDMS method is very similar to the proposed method in this paper, but the mounting positions of the camera differ significantly from the IBDM due to the elevation over the rotor disk.

Projection Methods

An alternative to the SPR methods are projection methods. These methods need a single camera and a device to project a grid onto the rotor. The set-up and angles of the projector and camera relative to the rotor and to each other are crucial. There are two very similar methods. The Fringe Correlation Method (FCM) also known as Projection Grid Method (PGM) [3] and the Projection Moiré Interferometry (PMI) [8]. In comparison the FCM is regarded to have a better accuracy while it is more sensitive to image noise due to particles on the blade surface [3]. An application in flight test is difficult regarding the changing visual conditions and the distance needed for both projector and camera relative to the rotor plane.

Conventional Rotor Blade Instrumentation

For in-flight rotor blade deflection measurements highly instrumented blades with strain and acceleration sensors can be used [9] [10]. For this purpose, an instrumented set of rotor blades needs to be built and the instrumentation calibrated. However, the acquisition of the measurements can be hindered, if there is not much space to mount a slip ring or to mount telemetry for data transfer. This hurdle is likely for overlapping rotors in the case of small drones as considered in this paper. Generally, the usage of instrumented rotor blades is a resource-intensive way to measure blade deflections. Furthermore, due to the instrumentation process the mechanical properties can change in comparison to production blades.

To counteract the difficulties of these methods applied to small-scale drone helicopters and to improve on the aspect of in-flight measurement, the following method to determine rotor blade deflection was developed.

BASIC PRINCIPLE

The basic set-up of the proposed measurement method is shown in Figure 1. It uses a single in-plane-mounted camera depicting the rotor blade while it is rotating. The camera is mounted at the rotor head assembly or the blade grip. Consequently the method is named In-Plane Blade Deflection Measurement (IBDM).

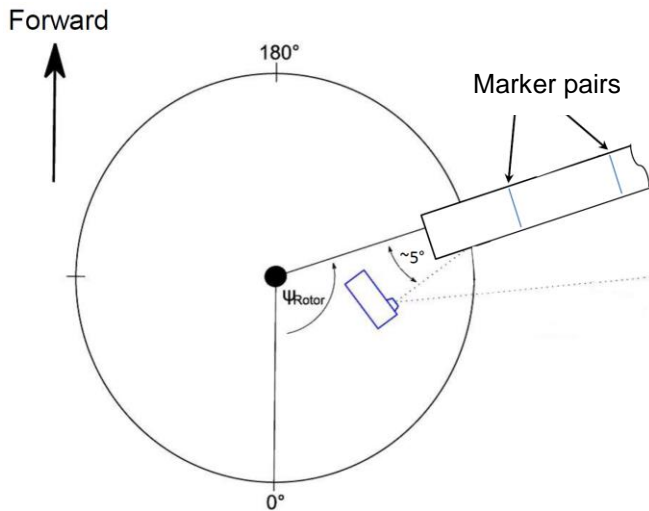


Figure 1 – Concept layout, top-down view [11]

Due to the camera position a shallow tilt angle of the camera of about 5° forward and upwards is needed relative to the rotor blade surface. These angles are needed to ensure the visibility of the marker pairs during blade motion, therefore these angles can change due to the magnitude of the expected blade motion. Optical marker pairs are introduced mounted perpendicular to the blade surface. The marker size can vary depending on the feature tracing algorithm used. In this test set-up the markers have a height and width of 8 mm (about 10% of the profile length) and are made from aluminum. Each marker pair is mounted at a pre-defined radial position and consists of a marker at the leading edge of the rotor blade profile and one at the trailing edge. The leading and trailing edge markers of a marker pair are connected with a supporting bridge which provides the mounting surface to the blade. The marker pairs are glued to the blade surface. The position of the camera and the arrangement of the markers are designed to measure a flap angle of at least 9° at any radial position.

The arrangement is chosen such that the overall measurement accuracy of the different markers stays as constant as possible. Therefore the optical distance between the leading and the trailing edge markers stays the same at the different radial positions. In Figure 2 the camera view is shown and the different marker pairs are enumerated in direction of the rotor blade tip. From one pair of markers the torsion angle

and the lead-lag and flap displacement can be calculated at its radial position.

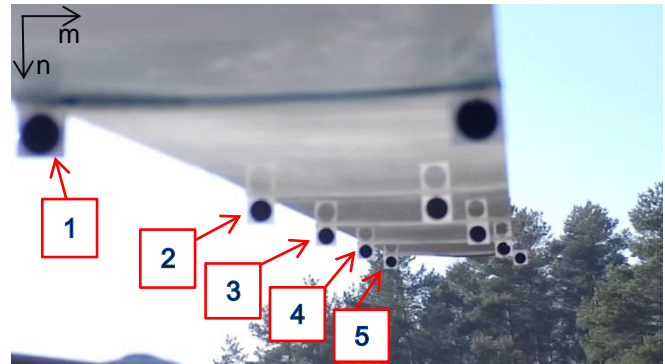


Figure 2 - Camera picture with rotor blade markers (leading edge markers are enumerated) and picture coordinate system

It has to be noted that the amount of markers per rotor blade cannot be increased arbitrarily due to the aerodynamic distortion caused by the markers themselves. Thus, the amount of distortion has to be balanced with the desired radial resolution. Such balancing can be achieved by defining the radial resolution needed and comparing the trim conditions with and without the instrumented blades for the flight condition in the scope of the study. An example is given in the chapter validation of this paper.

The camera mounting position is a crucial design decision. It defines the amount of additional measurement equipment needed to determine static and elastic blade deformation:

- The elastic blade deflection should be measured with a blade grip mounting. No additional sensors are needed for this measurement.
- In case of a measurement of the blade deflection in the helicopter frame a mounting of the camera at the central part of the rotor head should be chosen. With this mounting position only one additional sensor is needed to determine the rotor mast bending.
- For the measurement of both the elastic deflection and the deflection in the helicopter frame both mounting positions can be used, however the amount of additional sensors differs. In case of a blade grip mounting the commanded blade pitch angle as well as the displacement of the blade grip should be measured in order to determine the blade deflection in the helicopter frame. Here the blade grip displacement is a combination of the displacement of the rotor mast and the blade grip due to bending. If a mounting at the central part of the rotor head is chosen to measure the elastic blade deflection the rotor mast bending and the

commanded blade pitch angle are the additional measurements needed.

Circle detection is used to determine the marker positions within the images. Marker geometry and size and the used detection algorithms have an impact on robustness and accuracy. Other very important aspects are the sampling rate and the resolution of the cameras. Here lays a major strength of this method. The close proximity of the camera to the markers improves the measurement accuracy compared to most other optical methods having bigger camera-to-marker distances.

Experimental set-up of the superARTIS

The superARTIS is a DLR-operated intermeshing unmanned helicopter with a maximum take-off weight (MTOW) of 85 kg. It is equipped with a flight test instrumentation for structural and flight performance analysis [12].

In the experiments with the superARTIS helicopter two cameras were used on one of the two rotor heads, see Figure 3. For an azimuth reference marker the upper strobe light was modified.

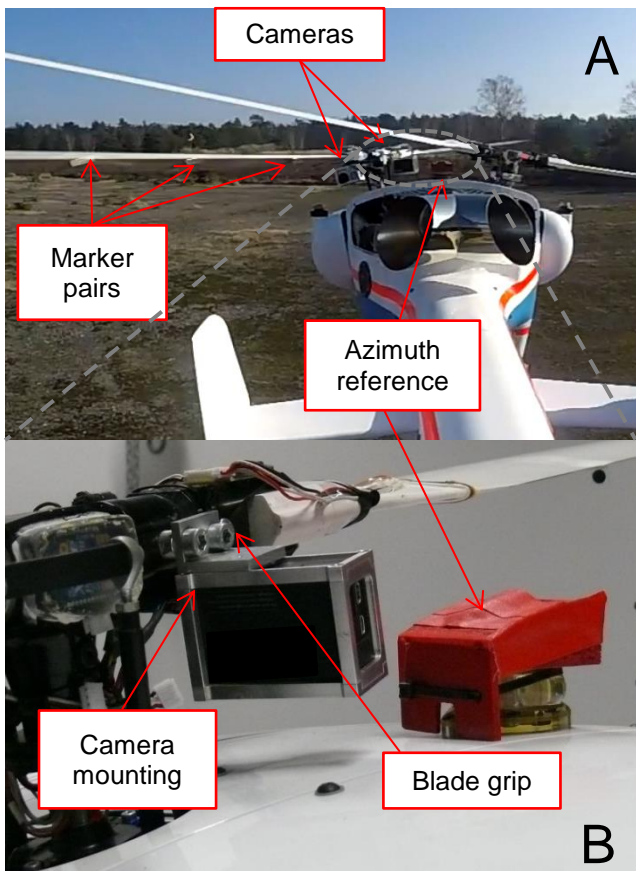


Figure 3 – Experimental set-up of the superARTIS; A in-flight picture; B details of the IBDM set-up

For this experiment the cameras were mounted at the blade grip of the left rotor. One reference marker was

used to determine a reference azimuth position. The rotor blades of the left rotor were each equipped with five marker pairs.

For validation additional sensors are used to measure the bending of the rotor mast and the blade grip. The blade grip flap angle was indirectly determined via a strain gauge measurement at the blade root, see Figure 4. These strain measurements are calibrated to provide the lateral displacement Δx of the rotor head, the elastic mast bending angle β_{Mast} as well as the elastic bending angle $\beta_{Blade\ grip}$ of the blade grip.

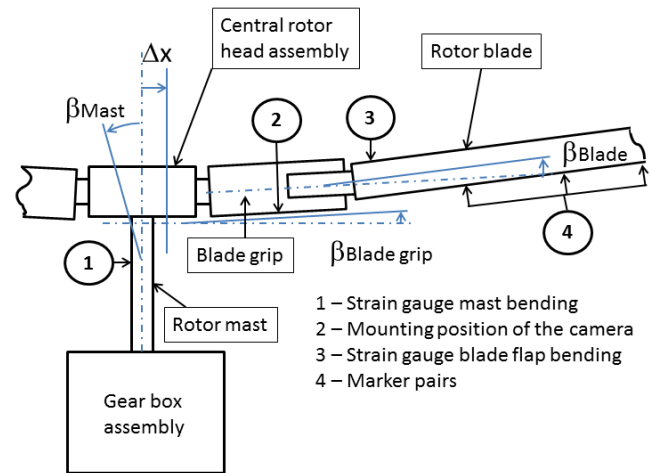


Figure 4 – Assumed motions of rotor head with correlating measurements

For later calculation of the blade pitch angle the actuator positions are determined and logged during the experiment. Instead of the not measured actuator positions, the commands are used as approximations.

The resolution of the cameras is 1280x720 pixels at a frame rate of 240 fps. This frame rate results in about 15 pictures per revolution for the superARTIS at the nominal rotor speed. The rolling shutter of the cameras is sufficient for this application, since the relative motion of the blade is sufficiently slow to not cause image distortion.

In the post processing of the images a correction with the intrinsic camera parameters is performed. On that corrected image an edge detection algorithm is used resulting in a black and white image. Afterwards, the marker detection is achieved via a circle detection algorithm based on “Circle Hough Transformation” (CHT) [13]. The identification of the markers is done by an estimation of the marker positions prior to image processing.

For later calculation of the blade deflections, reference marker positions are determined. These reference positions are needed in the process to define a reference blade deformation. For an absolute blade deflection, the reference positions of the markers need

to be determined in a non-deformed state of the rotor blade at the nominal rotor speed. For the validation experiments of the IBDM the reference positions were determined during a ground run at nominal rotor speed and without cyclic inputs as well as collective angles at close to the zero-lift angle of attack. These conditions were maintained for 60 seconds and a 16 second part is chosen in post processing where the variance was lowest. Over these 16 seconds averages of all sample points for each single marker are used as the reference position of this marker.

Coordinate Transformation

To calculate the rotor blade deflection several coordinate transformations are needed.

Firstly, a transformation from the image coordinate system to the camera coordinate system is necessary. Here, the intrinsic camera parameter matrix M_{int} is used and was determined with the "DLR Calibration Detection Toolbox" (DLR CalDe) and the "DLR Calibration Laboratory" (DLR CalLab) [14].

With the known marker positions m, n in the image coordinates a solution was calculated using:

$$(M_{int})^{-1} \cdot Z_c \cdot \begin{pmatrix} m \\ n \\ 1 \end{pmatrix} = \begin{pmatrix} X_c \\ Y_c \\ Z_c \end{pmatrix}, \quad (1)$$

with X_c, Y_c, Z_c denoting the unknown camera coordinates of the marker as shown in Figure 5.

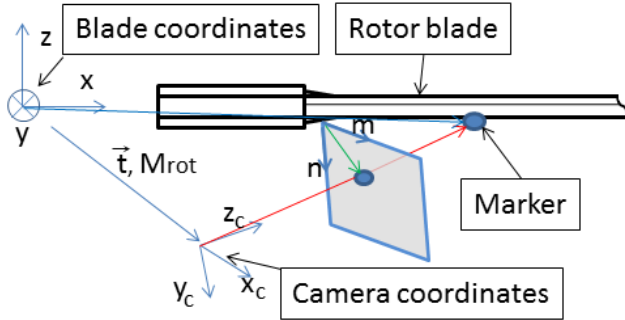


Figure 5 – Coordinate transformations from image to camera coordinates and from camera to blade coordinates

The second transformation translates the camera coordinates to the blade coordinate system. This blade coordinate system is blade grip fixed and the origin moved to the rotational center of the rotor in case of a not deflected blade grip. For the transformation a rotation of the coordinates is performed together with a translation

$$\vec{X} = M_{rot} \cdot \vec{X}_c + \vec{t}. \quad (2)$$

Both, the rotation matrix M_{rot} and the translation vector \vec{t} can be calculated via a CAD model of the rotor

assembly including the camera mounting. Another way is the calculation of the translation vector from a calibration as it is subsequently described.

In Figure 6 the transformation process is depicted. The deflected profile is depicted with the dotted line and the reference deflection is represented by the solid line profile. The shear center is marked as a dot. Here, d_{LE} denotes the center position of the leading edge marker relative to the shear center and respectively d_{TE} to the trailing edge marker.

To determine the blade deflection the torsion angle at each radial position ($i = \{1,2,3,4,5\}$) of the blade is calculated using

$$\Phi_i = \arctan\left(\frac{z_{LE_i} - z_{TE_i}}{y_{LE_i} - y_{TE_i}}\right) \quad (3)$$

The reference torsion angle is accordingly determined from the reference positions.

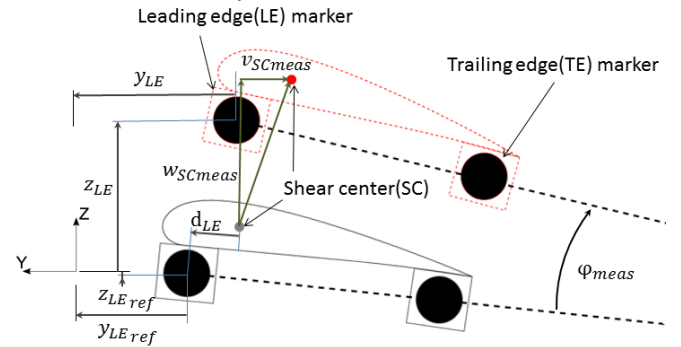


Figure 6 – Calculation of blade deflection

The torsion angle is corrected with the torsion angle of the reference marker pair positions according to

$$\Phi_{meas_i} = \Phi_i - \Phi_{ref_i}. \quad (4)$$

The leading and trailing edge markers are used to calculate the measured lead-lag v_{SCmeas} and flap displacement w_{SCmeas} . Therefore, the displacement of the shear center is calculated from both the leading and the trailing edge markers with the following formulas:

$$\begin{aligned} w_{SCL_i} &= z_{LE_i} - z_{LE_{ref_i}} \\ &- d_{LE_i} \cdot (\sin(\Phi_{meas_i} + \Phi_{ref_i}) - \sin \Phi_{ref_i}) \end{aligned} \quad (5)$$

$$\begin{aligned} w_{SCTE_i} &= z_{TE_i} - z_{TE_{ref_i}} \\ &+ d_{TE_i} \cdot (\sin(\Phi_{meas_i} + \Phi_{ref_i}) - \sin \Phi_{ref_i}) \end{aligned} \quad (6)$$

$$\begin{aligned} v_{SCL_i} &= y_{LE_i} - y_{LE_{ref_i}} + d_{LE_i} \\ &(\cos(\Phi_{meas_i} + \Phi_{ref_i}) - \cos \Phi_{ref_i}) \end{aligned} \quad (7)$$

$$\begin{aligned} v_{SCTE_i} &= y_{TE_i} - y_{TE_{ref_i}} - d_{TE_i} \\ &(\cos(\Phi_{meas_i} + \Phi_{ref_i}) - \cos \Phi_{ref_i}) \end{aligned} \quad (8)$$

The actual “measured” values of the displacements of the shear center in flap and lead-lag direction are taken as the respective means

$$w_{SCmeas_i} = \frac{w_{SCL E_i} + w_{SCT E_i}}{2} \quad (9)$$

$$v_{SCmeas_i} = \frac{v_{SCL E_i} + v_{SCT E_i}}{2} \quad (10)$$

Azimuth Determination

For the measured blade deflection data of each image an azimuth position needs to be determined. There are several ways of getting the azimuth information:

- Triggered camera pictures at certain angles
- Optical markers fixed to the helicopter
- Other signals logged as data in the camera (electrical, acoustic, ...)

These technical solutions can be challenging to implement. For the superARTIS a mounting of a slip ring or other technical solutions to electrically trigger the camera was not possible, therefore a robust and azimuth-accurate camera trigger was not implemented. Instead a combination of one visual marker (Figure 3) and a rotation sensor is used to determine the azimuth position during post-processing the data. Due to the limited angle of view of the camera, most images (typically 14 of 15 in this case) do not contain the marker. So a two-step approach is necessary: First, the images containing the marker have to be identified and the azimuth angles for these images have to be determined. Second, based on the rotor speed and the frame rate of the camera, the azimuth angles for the intermediate images (i.e. those without the marker) have to be determined. To detect the marker the camera images are filtered specifically to enhance the contrast for the marker (red colored marker). The transformation of the detected azimuth reference marker position to blade coordinates is performed analogously to the rotor blade marker transformation.

With the information given in this chapter the blade deflections can be calculated relative to a certain reference condition, e.g. a hover flight or an unloaded ground run. However, if a blade deflection measurement relative to a helicopter-fixed coordinate system is needed the motions of the camera mounting and the rotor mast are important as well. For this case, a set of transformations to rotor head- and helicopter-fixed frames is necessary.

CALIBRATION

The IBDM sensors, i.e. the cameras and the strain gauges, needed to be calibrated.

First, the determination of the intrinsic camera parameters was performed using a calibration pattern and the Software CalDe and CalLab, mentioned

earlier. In this calibration step a known calibration pattern is used to create correction parameters for optical distortion caused by the lens and camera sensors used.

Second, the calibration of the azimuth reference was done by manually rotating the rotor on the ground until the marker position was located central in the image taken by one of the cameras. The azimuth position where the azimuth marker was detected to be central was manually measured and determined several times. The azimuth angle from the manual measurement and the azimuth angle from the marker detection were compared and consequently the marker detection corrected.

Third, a static calibration of the strain gauges was done. The strain gauges are located at two positions. At the rotor mast to measure the rotor mast bending and at the blade root to measure the blade flap bending. In a static calibration procedure 25-30 calibration points were measured for each sensor. During the calibration one blade was used to apply a vertical force at 500 mm from the rotor center. The blade pitch angle was chosen to be 0° resulting in a pure blade flap bending and mast bending load. The determined measurements can be found in Figure 4.

ACCURACY AND COMPARISON TO OTHER METHODS

The accuracy of this method is determined by the properties of the cameras, markers and mounting set-up used to measure the blade deflection.

The overall accuracy is a result of several potential measurement uncertainties and errors. First, the remaining measurement uncertainty of the cameras depends on the camera parameters and the calibration approach itself. In general, an RMS error of 0.5 to 0.1 pixels is achievable for the intrinsic parameters of the cameras. The calibration RMS error for both cameras used in this experiment was 0.163 – 0.165 pixels.

Another source of measurement uncertainty is the detection of the markers. Generally it is recommended to choose a marker area resulting in at least 10 pixels to ensure a sufficiently accurate detection of the markers. Such markers are detectable to a subpixel accuracy of down to 0.1 pixels [15]. However this is more the theoretic value. With the marker detection approach and the markers used in this set-up an error of 0.5 pixels was estimated by manually checking the detection result with the manually measured results.

The accumulated measurement accuracy of all sources will vary from the theoretic value of 0.1, the best marker detection accuracy assumed and the other errors negligibly small, to more realistic 0.7 pixels. In

the example of the superARTIS an accumulated measurement accuracy of 0.675 pixels is estimated.

The determined measurement accuracy for the different marker pairs together with detailed information regarding marker size and marker position can be found in Table 1.

Table 1 – Geometry data and measurement accuracy per marker pair

Marker pair	1	2	3	4	5
Relative radial position [position/rotor radius]	30%	50%	65%	80%	95%
Radial position [mm]	433	722	938	1154	1371
Distance between markers front/rear [mm]	81	61	71	81	91
Marker radius [mm]	4	4	4	4	4
Marker radius [pix.]	42	19	13	10	8
Spatial resolution [mm/pix]	0.095	0.21	0.31	0.4	0.5
Accuracy flap & lead-lag displacement [mm]	0.064	0.14	0.21	0.27	0.34
Accuracy torsional deflection [°]	0.091	0.27	0.34	0.38	0.43

In Table 2 a comparison of other blade deflection measurement methods in terms of accuracy and statistical measurement error is shown. This comparison is based on the published data of the references given in the last column. The accuracy is either given as a simulated value or was estimated during the development process as part of the validation process by the authors of the publications. In one case the error was estimated from the measured data and the estimated accuracy is given as two times the standard deviation provided by the authors of this paper.

The measured error of the IBDM is given as two times the standard deviation of the error (covering 95.4% of all samples assuming a normal distribution). The data for the IBDM was sampled during a ground run with constant actuator positions and at wind speeds below 2 m/s. This method has not yet been tested in wind tunnel, as it is the case for the other methods. Therefore the data used to estimate the statistical error of the IBDM is more influenced by changing environmental conditions during the validation tests. Therefore, the statistical errors calculated for the IBDM can be considered as nominal to worst case estimation.

The IBDM approach shows relative to the other methods a good overall accuracy for the flap and lead-lag displacement. This can be explained by the high camera resolution and the short distance between

marker and camera leading to a resolution per marker of at least 200 pixels.

Table 2 – Accuracy comparison of different methods

Method	Theoretical best Accuracy [pix. or %]	Estimated/measured absolute error in mm/rotor radius or %rotor radius		Sensor set-up	Ref
		Flap/Lead-Lag [mm/m]	Torsion [°/m]		
SPR	1/10	0.2	0.26	4x 1280x1024	[15] [16]
	1/10	0.455 to 1.36	-	-	[17]
FCM	1/20	0.476	0.143	1x 768x512	[3]
PMI	1/10	0.35 to 1.16	0.26	1x 640x240	[8]
BDMS	~1/10	0.11 to 0.2	0.03 to 0.04	2x 768x576	[5]
SPA	3,5%	0.7 to 1.3	0.3 to 1.3	25 gauges	[10]
IBDM	1/10	0.12 to 1.2	0.045 to 0.26	1x 1280x720	

The general set-up is very similar to the more accurate BDMS method. Although the resolution of the tested camera of the BDMS is at least 25% (in n-direction) lower the overall accuracy is higher compared to the IBDM. The magnitude of the accuracy difference seems to be quite high and cannot entirely be explained by a more accurate and robust marker detection. However the reasons for the good results of the BDMS could not be clarified in this paper.

For torsional deflection, the IBDM does not perform as well as the other methods. The determination of the torsion angle is more sensitive to errors in the marker detection than the determination of flap or lead-lag displacements. For example in the calculation of the flap displacement a mean value of both markers is used. The torsion angle is calculated from the difference of the leading and trailing edge markers. Thus inaccurate marker detection is more apparent in the relative error of the torsion angle than in the flap or lead-lag measurement with regards to the marker distance used.

It is also apparent that the spread of the measurement accuracy is higher than that of the other methods. This spread can be caused by the marker detection algorithm and lighting effects. This is an indication that the marker detection algorithm should be improved in terms of robustness.

The IBDM set-up can influence the aerodynamic and mechanic behavior.

The aerodynamic influence of the markers on the blade motion especially in forward flight is difficult to assess. The size and number of markers on the rotor blades should be chosen carefully. In this paper a more detailed analysis of those effects is given, see the validation chapter. If the IBDM is used in tests with significant forward flight speeds the aerodynamic influences of the markers will increase due to the radial flow components over the rotor blades.

The increase of torsional and bending stiffness of the blades due to the mounting of the marker pairs was not directly measured. It is considered to be negligible because the stiffness of the blades is significantly higher than the additional stiffness due to the markers.

The additional weight of the camera will have an impact on the torsional moment of inertia of the blade and the blade grip. It was estimated that the additional mass doubles the moment of inertia about the torsional axis. This significantly changes the torsional natural frequency and should be taken into account. For this proof of concept however, these changing characteristics were not in the scope of the study.

Another potential cause of measurement error is the stiffness of the camera mounting. To evaluate the influence of the stiffness of the camera mounting a static measurement was done. The centrifugal force is the main loading for the camera which has to be considered. Therefore a static and equivalent loading corresponding to the centrifugal force was applied. In the test the camera was used to depict the instrumented blade. The images were processed as described beforehand with the unloaded camera images used as the reference positions. During that measurement a 0.22° angle displacement was observed between the unloaded and loaded condition. This offset was accounted for the azimuth angle.

VALIDATION

To validate the method a ground run and a flight test have been conducted.

An estimation of the aerodynamic influence of the markers on the rotor was done using the following experiment: The helicopter was trimmed in hover condition using an unmodified set of rotor blades. Afterwards, the helicopter was equipped with one modified set of rotor blades (one of the two rotors). Using the same actuator positions previously determined, the helicopter motion was assessed. In essence, there was no drift apparent indicating that the aerodynamic effect of the markers is negligible in an average sense for hover.

The data of the same flight test was used to measure the power consumption of both rotors with strain gauge and revolution per minute measurements [12]. The

comparison of the data with and without the IBDM modification shows no measurable difference. For this power consumption instrumentation an error of less than 2% can be assumed according to the design and calibration of the involved sensors. During high speed flights with pronounced transverse flow an assessment of the aerodynamic influence needs to be performed if the IBDM will be applied for significant forward flight speeds.

To validate the accuracy of the data measured by the IBDM a reference measurement with strain gauges of the blade flap angle at the blade root was used. During a ground run a moderate cyclic input was given and the IBDM and the strain measurements were compared, see Figure 7.

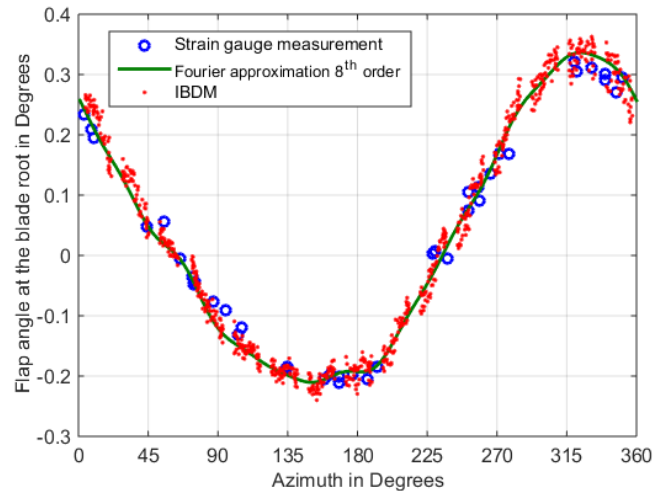


Figure 7 – Comparison of the blade flap angle with a strain reference measurement

In Figure 7 the dots and circles show the measured flap angles at the blade root for the IBDM and the strain gauge measurements. Both data sources are sampled for about 30 rotor revolutions. In comparison both measurements show the same general characteristics and the spread of the data is very similar as well.

The blue markers represent flap angle estimations based on the strain gauge measurements. The red markers have been measured using the first marker pair (at 433 mm) of the IBDM. This blade deflection information was used to calculate the angular deviation at the blade root where the strain gauge measurement is located. The green line is the used approximation for the IBDM data. The strain measurement was statically calibrated to measure the flap angle prior to this test. Please note that a different bending moment distribution during the test compared to the calibration can cause measurement inaccuracy. To minimize the effect of additional bending moments resulting from higher eigenmodes or disturbed load distributions a ground test was chosen with moderate cyclic inputs and minor rotor thrust.

To check the robustness and the accuracy of the IBDM a blade to blade comparison was done, see Figure 8. The data shown in Figure 8 are sampled at the same ground run from the markers at a rotor radius of 1.369 m. The error bars show two times the standard deviation. The lines of the blade deflection are a Fourier approximation of 8th order. The data was sampled over about 30 revolutions.

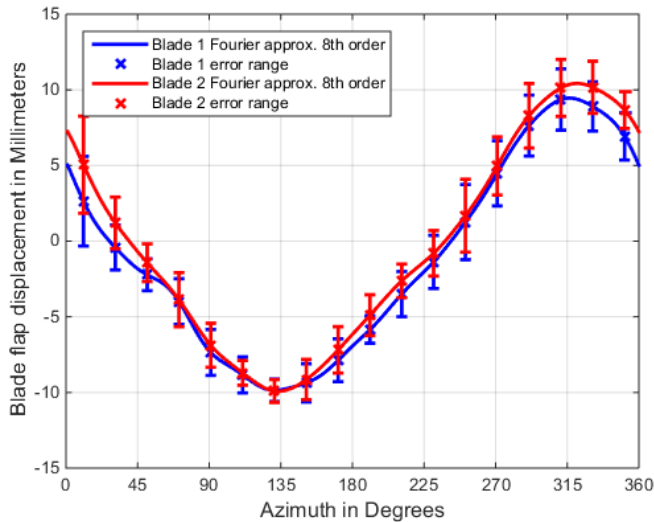


Figure 8 – Blade to blade comparison during ground run; marker pair at 1.369 m rotor radius

A direct comparison of both blade deflection measurements shows a very similar behavior and general characteristics of both measured blade deflections.

RESULTS OF THE METHOD

The following data was acquired during a test campaign to demonstrate the proof of concept for the IBDM.

First, a ground run was performed with unloaded rotor to sample data to calculate the reference position of the markers. Following the phase to sample the reference data a moderate cyclic command input was given to determine flap phase lag of the blades and to sample data for validation.

Second, two flight tests of the superARTIS were conducted in hover to slow level flight. During the first flight the IBDM set-up was used to measure blade deflection data. The second flight was done without the instrumented blades to verify the influence of the blade markers.

The IBDM measurement set-up worked without technical difficulties. There was no blade deflection measurement for the right rotor.

In the following the data for a forward flight condition is presented. The following plots are approximations of the sampled data. In terms of radial approximation a third-order polynomial function is used and in azimuthal dimension a Fourier approximation of 8th order is used. The plotted radial range is from 0.433 to 1.369 m.

The blade root at 0.2 m and the blade tip at 1.442 m are marked with a grid line. The radial locations of the blade markers are marked in the plot with dashed grid lines. The collective pitch angle Θ_0 as well as the lateral Θ_C and longitudinal Θ_S pitch angles are used defined as defined in [18] page 24.

In Figure 9 the blade flap displacement during a slow level flight is presented. The flapping motion of the rotor blades is clearly dominated by a large flapping displacement at about 180° - 320° and a small flapping displacement on the opposite side of the rotor.

$$\mu=0.035 \quad \mu_z=0 \quad C_T/\sigma=0.106 \quad \theta_0=7.1^\circ \quad \theta_S=0.1^\circ \quad \theta_C=-0.44^\circ$$

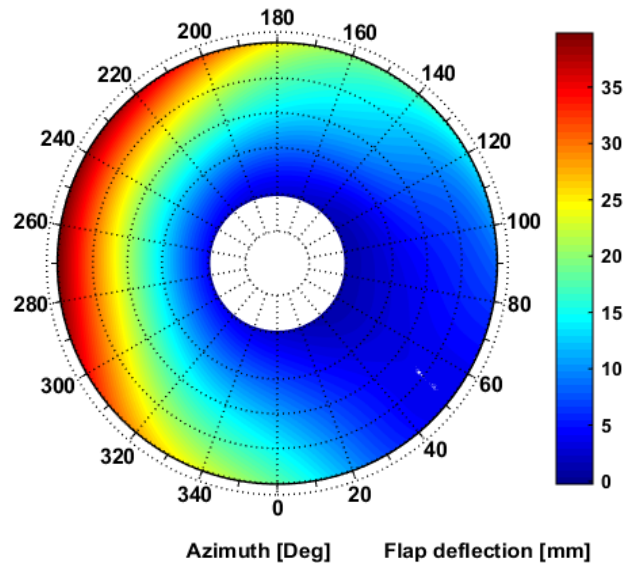


Figure 9 - Blade flap displacement during slow level flight

The flap displacement during this close to hover flight condition can clearly be measured and shows a much bigger magnitude than the expected measurement accuracy of about ± 1.18 mm. In Figure 10 a comparison of both blades is illustrated together with the error range of the measured data based on the standard deviation as described before. Please note that the error range comprises beside the measurement noise also the changing pitch angles to compensate for disturbance since the data was samples during a period of 3 seconds.

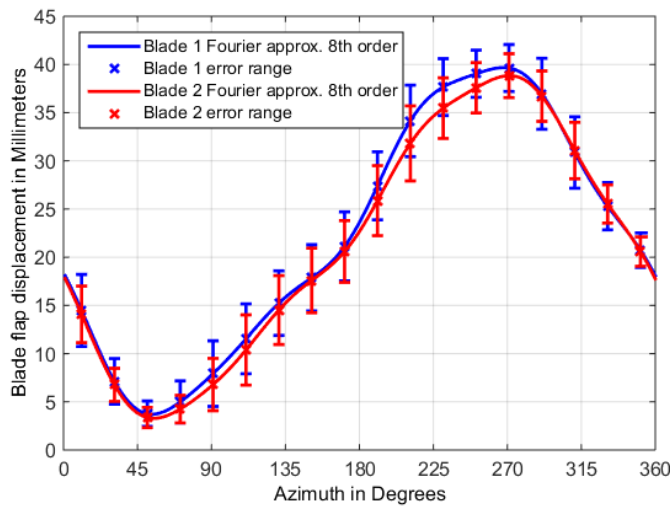


Figure 10 – Blade to blade comparison of flap displacement in slow level flight; marker pair at 1.369 m rotor radius

The blade to blade comparison shows the same general characteristics compared to the ground run discussed before. The data sampled with the IBDM is consistent for both blades in spread of the data as well as blade displacement magnitude. The data is also consistent in radial direction, see Figure 11. For validation purposes it can be assumed that the main component of the blade flap motion is the first eigenmode, therefore the data should show a flap blade displacement close to a linear function over the rotor radius.

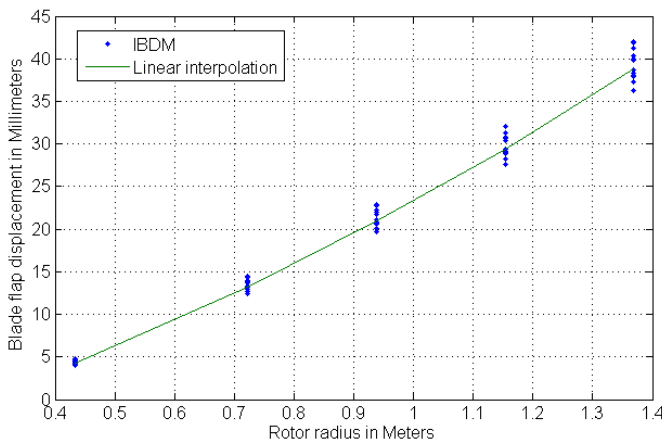


Figure 11 – Blade flap at 270 degrees azimuth angle

Generally, the measured blade flap displacement with the IBDM shows a valid behavior in blade to blade comparison and in radial direction for tested flight condition. Thus the IBDM can be considered as a usable method to determine flap displacement during flight and ground test.

The lead-lag displacement during the same flight condition is presented in Figure 12.

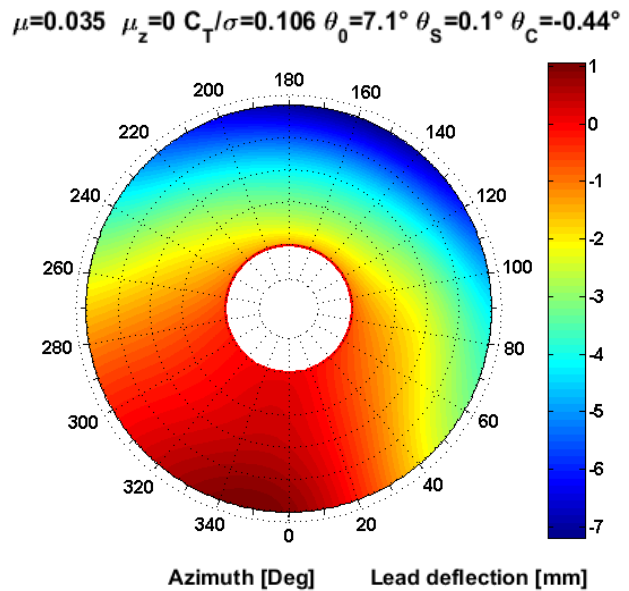


Figure 12 – Blade lead-lag displacement during slow level flight

A mostly negative lead motion was measured with a pronounced lag at the front side of the rotor disk. The data in blade to blade comparison also show a consistent and valid blade motion (not presented in this paper). Therefore, it can be assumed that the IBDM is a robust method to measure lead-lag displacement.

The error of the torsional deflection was higher in the analytical and statistical analysis compared to the other methods. The measured standard deviation of the used test data is up to 0.38° for the elastic blade torsion for both of the measured rotor blades. A comparison of torsional deflection of both blades is given in Figure 13. Although the estimated error is relatively high compared to the magnitude of the signal, a clear blade motion of both of the blades is apparent.

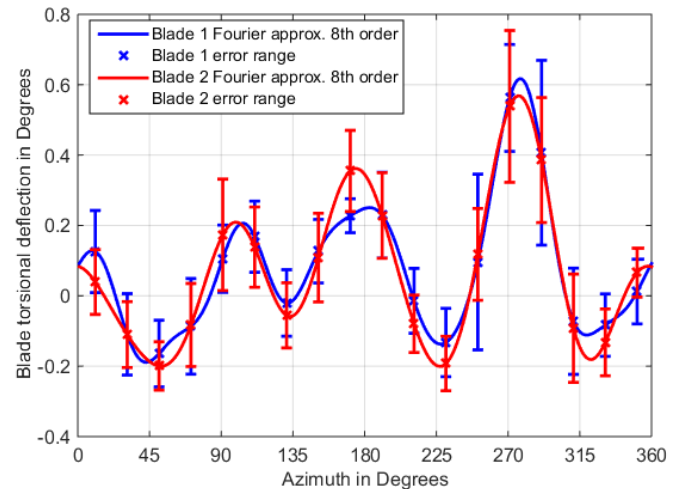


Figure 13 – Blade to blade comparison of torsional deflection in slow level flight; marker pair at 1.369 m rotor radius

The torsional deflection over the rotor disk is presented in Figure 14.

$$\mu=0.035 \quad \mu_z=0 \quad C_T/\sigma=0.106 \quad \theta_0=7.1^\circ \quad \theta_S=0.1^\circ \quad \theta_C=-0.44^\circ$$

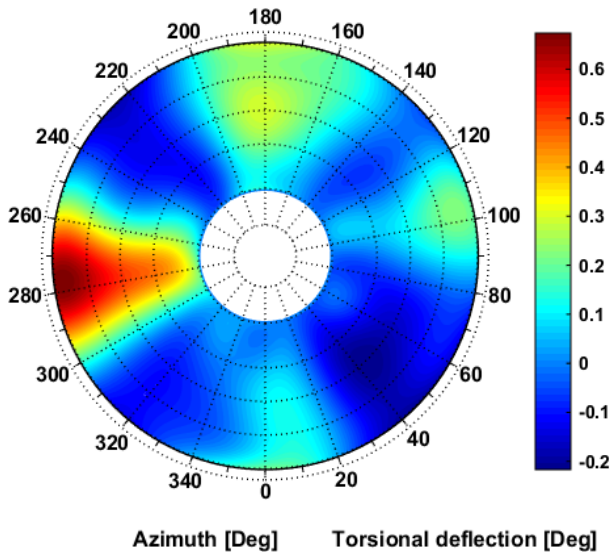


Figure 14 – Blade torsional deflection during slow level flight

Considering the error range of the data it can be said that the general characteristics and the magnitude of torsional deflections can be determined with the IBDM. However, an improvement of the measurement accuracy of the torsional deflection should be considered if the IBDM is applied. It is recommended to use the full length of the blade chord to increase the distance of the leading and trailing edge markers.

The overall errors determined for the in-flight measurements can be found in Table 3. Please note that the measured standard deviations presented in Table 3 are calculated over a 3 second interval and they are not compensated for blade deflection due to changing control inputs.

Table 3 – Overview of the measured standard deviations

	Min.	Max.	unit
Flap	0.6	4.9	mm
Lead-Lag	0.38	2.19	mm
Torsion	0.1	0.38	°

CONCLUSION

The IBDM was successfully tested to determine flapping, lead-lag and torsional motion of rotor blades. The approach is easy to understand and relies on a single camera per rotor blade depicting the blade while in motion. The rotor blades are equipped with markers. In the experiments presented, the influence of the markers on the aerodynamic characteristics was found

to be sufficiently small. Nevertheless, if different marker or blade dimensions are used, the influence has to be assessed anew.

The accuracy for lead-lag and flapping motion is comparable to existing methods. Only the torsional accuracy is worse than the existing methods.

Depending on the mounting position of the camera, the measurement data need to be corrected for mast bending and/or the motion of the blade grip. For a determination of the elastic blade deflection a set-up consisting of a camera and an azimuth marker is sufficient.

The application during flight test and the straightforward approach are strengths of the presented method.

One major drawback of the method as for all optical in-flight methods is the susceptibility to the changing visual environment. Especially if the markers are exposed to direct sunlight and therefore a changing shadow on the markers the detection quality can degrade. However, an increase in robustness of the marker detection is surely achievable considering the very basic algorithms used here.

In summary, the IBDM is a simple and generally reliable means to measure the blade deflection. The IBDM can be used especially, if mounting constraints or rotor configurations with significant rotor overlap do not allow the use of other methods.

In the future an assessment of the influence of the markers on the rotor aerodynamics in fast forward flight needs to be performed. Furthermore a more detailed assessment of the influence of the IBDM with regards to blade eigenfrequencies should be performed. The marker detection should be improved in order to mitigate the effect of direct lighting and to increase the overall robustness.

ACKNOWLEDGEMENT

The authors would like to thank our colleagues of the Institute and especially B.G. van der Wall and W. Mönnich for many fruitful discussions leading to a great improvement of this study.

REFERENCES

- [1] O. Schneider and B. G. van der Wall, "Final Analysis of HART II Blade Deflection Measurement," in *29th European Rotorcraft Forum*, Friedrichshafen, Germany, 2003.

- [2] A. I. Abrego, L. Meyn, A. W. Burner and D. A. Barrows, "Summary of Full-Scale Blade Displacement Measurements of the UH-60A Airloads Rotor," in *Technical Meeting of the American Helicopter Society*, San Francisco, CA, 2016.
- [3] R. Müller, K. Pengel and B. van der Wall, "Blade Deflection Measurement at the Low Noise ERATO Rotor," in *26th European Rotorcraft Forum*, The Hague, Netherlands, 2000.
- [4] J. Baqersad, T. Lundstrom and C. A. P. Niezrecki, "Measuring the Dynamics of Operating Helicopter Rotors and Wind Turbines using 3D Digital Stereophotogrammetry," in *69th Annual Forum of the American Helicopter Society*, Phoenix, AZ, 2013.
- [5] B. Bosnyakov, V. Kulesh, A. Morozov, N. Tarasov and S. Fonov, "Videogrammetric system for study of movement and deformation of real-scaled helicopter rotor blades," in *Proceedings of Twenty-Third International Congress on High-Speed Photography and Photonics*, Moscow, Russia, pp. 196–209, 1998.
- [6] T. R. Norman, C. Theodore, P. Shinoda, D. Fürst, U. T. P. Arnold, S. Makinen, P. Lorber and J. O'Neill, "Full-Scale Wind Tunnel Test of UH-60 Individual Blade Control System for Performance Improvement and Vibration, Loads and Noise Control," in *65th Annual Forum of the American Helicopter Society*, Grapevine, TX, 2009.
- [7] F. Boden and B. Stasicki, "Non-intrusive In-flight Propeller Blade Deformation Measurements by Means of a Rotating Camera," in *34th European Telemetry and Test Conference*, Nürnberg, Germany, 2014.
- [8] G. A. Fleming and S. Althoff Gorton, "Measurement of Rotorcraft Blade Deformation using Projection Moiré Interferometry," *Shock and Vibration*, vol. 7, no. 3, pp. 149-165, 2000.
- [9] R. M. Kufeld, D. L. Balough, J. L. Cross, K. F. Studebaker, C. D. Jennison and W. G. Bousman, "Flight Testing the UH-60A Airloads Aircraft," in *50th Annual Forum of the American Helicopter Society*, Washington, DC, 1994.
- [10] N. Tourjansky and E. Szèchényi, "The Measurement of Blade Deflections - A New Implementation of the Strain Pattern Analysis," in *18th European Rotorcraft Forum*, Avignon, France, 1992.
- [11] F. Knaak, "Entwicklung eines Verfahrens zur Bestimmung der aerodynamischen Kräfte aus der Rotorblattbewegung," RWTH Aachen, Aachen, Germany, 2017.
- [12] A. E. Voigt, J. Dauer, A. Krenik and J. S. Dittrich, "Detection of Forward Flight Limitations of Unmanned Helicopters," in *72nd Annual Forum of the American Helicopter Society*, West Palm Beach, FL, 2016.
- [13] T. Atherton and D. Kerbyson, "Size invariant circle detection," *Image and Vision Computing*. Volume 17, Number 11, pp. 795-803., 1999.
- [14] K. H. Strobl, "DLR CalDe and DLR CalLab," [Online], <http://www.robotic.dlr.de/callab/>.
- [15] K. Pengel, R. H. G. Müller and B. G. van der Wall, "Stereo Pattern Recognition - the technique for reliable rotor blade deformation and twist measurement," in *American Helicopter Society International Meeting on Advanced Rotorcraft Technology and Life Saving Activities*, Utsunomiya, Japan, 2002.
- [16] O. Schneider, "Analysis of SPR measurements from HART II," *Aerospace Science and Technology*, Vol 9 (2005), pp. 409-420, 2005.
- [17] L. E. Olson, A. I. Abrego, D. A. Barrows and A. W. Burner, "Blade Deflection Measurements of a Full-Scale UH-60A Rotor System," in *Aeromechanics Specialists' Conference of the American Helicopter Society*, San Francisco, CA, 2010.
- [18] W. Johnson, *Helicopter Theory*, Princeton, NJ : Princeton University Press, 1980.
- [19] R. H. G. Müller and K. Pengel, "Fringe Correlation Method for Helicopter Rotor Blade Deflection Measurement," in *24th European Rotorcraft Forum*, Marseilles, France, 1998.